Characterization of *cis*-1,4-Polyisoprene Polymerized with Lanthanide Catalyst System (Ln–PIR)*

QIAN BAOGONG (CHIEN, PAO-KUNG), YU FUSENG, CHENG RONGSHI, RUAN MEINA ZHANG WANJUN, LI SHENTIAN, ZHANG YANSHOU, and YANG YUHUA, *Changchun Institute of Applied Chemistry, Academia Sinica, People's Republic of China*

Synopsis

The PIR raw rubber samples, Ln–PIR and Ti–PIR, were subjected to molecular characterization, which shows that Ln–PIR contains microgel particles, but the least branching in its macromolecular chains; its *cis*-1,4 content is about 96% and molecular weight distribution is rather broad. The value of α in the Mark–Houwink viscosity equation for molecular weight M_η is determined as 0.70. The abnormal stress–relaxation behavior can be normalized by the introduction of an entanglement reduction factor, e.g., M_η/M_c for maximum relaxation time. This reduction is subsequently verified by evaluating the molecular weight dependence on bulk viscosity with 3.45th power. The starting of a yield process is equivalent to that of a disentanglement process, since both processes have approximately the same activation energy, 8 kJ/mol. For the onset of yield or of entanglement, the critical molecular weight M_c as estimated independently by yield strength method or by relaxation spectrum is equal to $(5.4 \pm 0.2) \times 10^4$. It is confirmed by the reduced yield strength method by calculating M_e from the equation $M_e = 3g_N\rho RT/E_{eN}$ with $g_N = 1.22$ and then by extrapolation, where E_{eN} is the equilibrium modulus due to entanglement.

INTRODUCTION

A series of polydienes polymerized with lanthanide coordination catalysts have been developed.[1] The *cis* content of *cis*-1,4-polyisoprene polymerized with rare-earth catalyst system (Ln–PIR) varies with rare-earth elements and the polymerization condition used, ranging from 93–98%.[1] And the *cis* content could attain 96.x% when mixed lanthanides was used. For example, examination with an infrared spectrometer (Perkin-Elmer IR 599B), ^{1}H- and ^{13}C-NMR (JEOL 100 NMR), shows that purified sample of Ln–PIR (C) contains 96.3% *cis*-1,4 and 3.7% 3,4-structural units, and there is no evidence of the existence of other units [Fig. 1(a),(b),(c)].

For characterization of the structural and viscoelastic properties of Ln–PIR raw rubbers, the methods used are similar to those reported for lanthanide catalytically polymerized *cis*-1,4-polybutadiene (Ln–PB).[2] For comparison, studies were also carried out on titanium catalytically polymerized polyisoprene (Ti–PIR) and natural rubber (NR), and some times on Ln–PB, so as to investigate the degree of linearity of macromolecular chains and the extent of entanglements in bulk.

* Presented before the Japan-China Bilateral Symposium on polymer Science and Technology, Tokyo, October 26–29, 1981.

Journal of Applied Polymer Science, Vol. 30, 375–390 (1985)
 CCC 0021-8995/85/010375-16$04.00

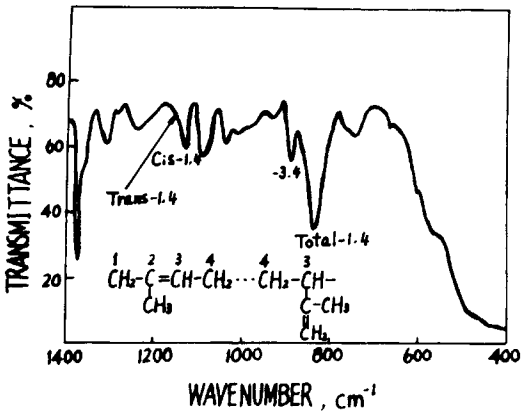

(a)

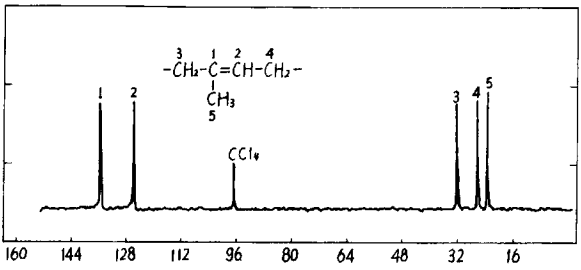

(b)

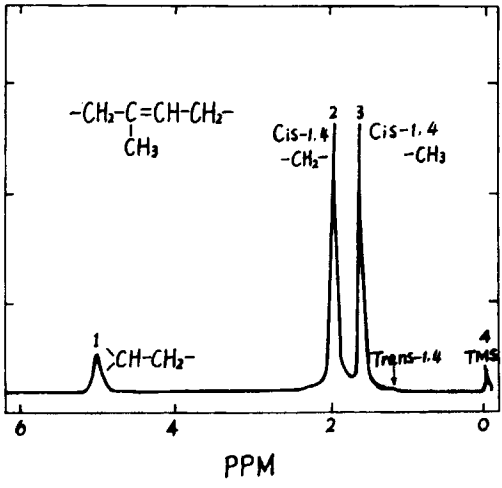

(c)

Fig. 1. (a) IR, (b) ^{1}H-, and (c) ^{13}C-NMR spectrum for purified Ln–PIR(GC).

Except for the determination of the viscosity $[\eta]$ equation for molecular weight M_η, all the bulk samples, either freshly polymerized or stored, used in the mechanical experiments, such as stress–relaxation and yield strength, were not fractionated. The determination of their $[\eta]$ or M_η was carried out with the same processed specimen right before mechanical testing, in order to avoid any possible structural difference caused by storage and/or by processing.

MOLECULAR WEIGHT AND MOLECULAR WEIGHT DISTRIBUTION

A Ln–PIR(J) sample was fractionated using toluene and methanol as solvent and precipitant, respectively. Like Ln–PB,[2] Ln–PIR contains microgels with catalyst particles as a central core. The amount of microgels in the rubber varies with the state of the catalyst. The Ln–PIR sample used in the present work contains a larger amount of microgels due to the heterogeneity of the polymerization system. Most of the microgels in the sample solution may be removed by $CaSO_4$ adsorption and high speed centrifugation (14,000 rpm) before fractionation. The weight average molecular weights and radius of gyration of the fractions were determined by light scattering using cyclohexane as solvent. In the higher molecular weight fractions there still remains a small amount of microgels, which behave like highly

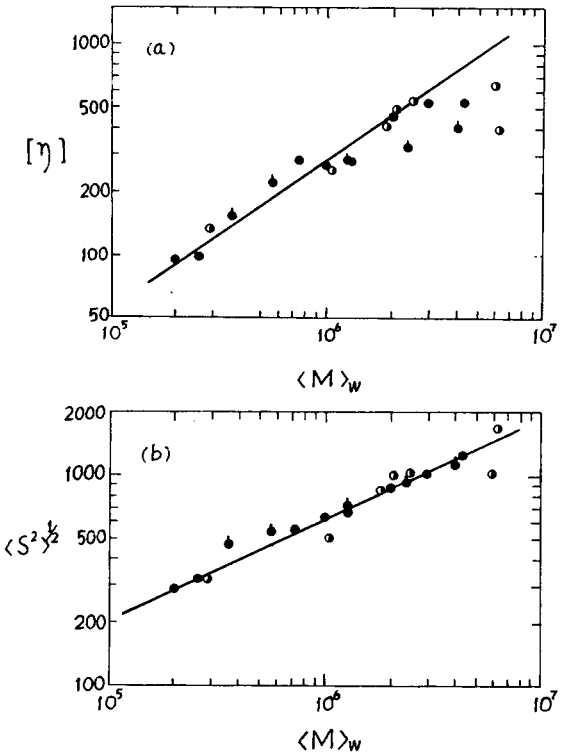

Fig. 2. Molecular characterization in dilute solution of PIR fractions: (a) log $[\eta]$ vs. log $\langle M\rangle_w$ plot [(●●)Ln–PIR(J); (◐)Ti–PIR(C)] (b) log $\langle S^2\rangle^{1/2}$ vs. log $\langle M\rangle_w$ plot.

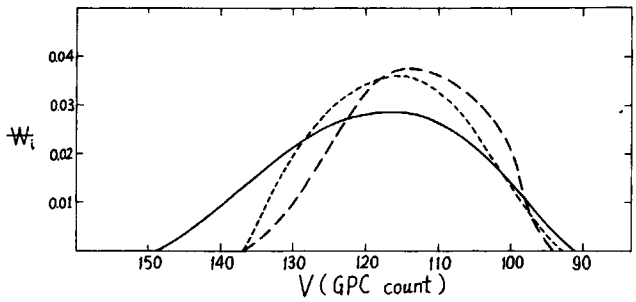

Fig. 3. The normalized chromatogram of PIR whole samples: (– –) Ln–PIR(J); (—) Ti–PIR(B); (- - -) Ti–PIR(C).

branched macromolecules, leading to a downwards curved Zimm plot in the region of low scattering angles[2] and thus giving higher molecular weights. The intrinsic viscosities of the fractions were determined in toluene. A Ti–PIR(C) sample was also fractionated and subjected to light scattering and viscosity measurements for comparison.

Since polyisoprene macromolecules are extremely sensitive to light and oxygen, all the fractionation experiments were repeated for checking. Antioxidants were added to the solution during fractionation and measurement of viscosity in toluene. For the light scattering measurement, the sample was precipitated from toluene solution and then redissolved in cyclohexane in order to increase the intensity of the scattered light; hence, antioxidant was removed. Therefore, the scattering of data points [Fig. 2(a)] might be due to preferential degradation of macromolecules of higher MW.[2]

The log–log plot of intrinsic viscosity $[\eta]$ vs. weight average molecular weight $\langle M \rangle_w$ is shown in Figure 2(a), in the lower molecular weight region. The relationship between intrinsic viscosity and molecular weight $[\eta](M)$ may be represented by the Mark–Houwink equation with an exponent value of 0.70,

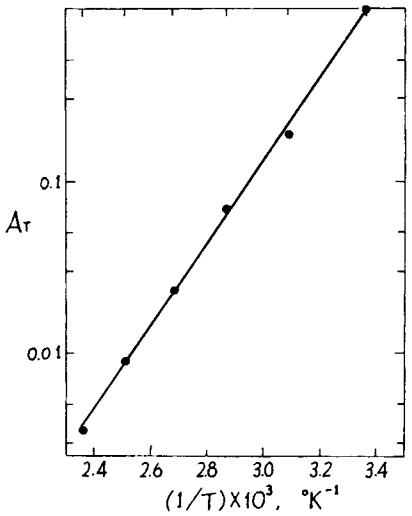

Fig. 4. Arrhenius plot of shift factor A_T against temperature $(1/T)$ for Ln–PIR(G5).

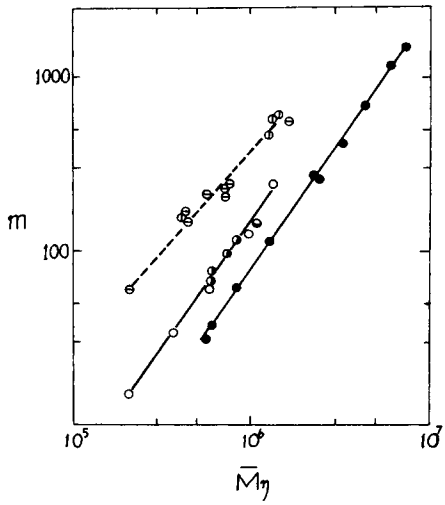

Fig. 5. Double logarithmic plot of number of entanglement segment m against viscosity average molecular weight M_η: (●) Ln–PIR; (◑) Ti–PIR; (◒) Li–PIR; (○, ○) data from literature; (○) NR.

$$[\eta] = 1.73 \times 10^{-2} \langle M \rangle_w^{0.70} \quad \text{(mL/g, toluene, 30°C)}$$

which may be considered as the characteristic correlation for linear polyisoprene. The relationship between radius of gyration $\langle S^2 \rangle^{1/2}$ and weight average molecular weight $\langle M \rangle_w$ [Fig. 2(b)] may be represented by

$$[S^2\rangle^{1/2} = 0.85 \langle M \rangle_w^{0.48} \quad \text{(cyclohexane)}$$

The exponent is 0.48, close to the theoretical value, 0.5.

The heterogeneity indexes of the fractions used are rather high (around 2); if both the effect of the polydispersity of the sample and that of the existence of microgels are considered, the monodisperse Mark–Houwink equation obtained for Ln–PIR is close to that obtained by Beattie and Booth (Table V), which will be presented in a subsequent article.

TABLE I
Molecular Characteristics of PIR Whole Samples

PIR sample	Gel[a] (%)	GPC[b] $\langle M \rangle_w \times 10^{-6}/\langle M \rangle_n \times 10^{-6} = \langle M \rangle_w/\langle M \rangle_n$			Intrinsic viscosity[c] $\langle [\eta] \rangle_{expt}/\langle [\eta] \rangle_{GPC} = \langle g \rangle_\eta$		
Ln–(J)	0.9	2.44	0.81	3.02	466	465	1
Ti–(A)	4.8	3.46	1.23	2.81	326	585	0.56
Ti–(B)	4.2	2.94	1.66	1.77	416	554	0.75
Ti–(C)	4.5	2.35	1.27	1.85	374	469	0.80
Ti–(D)	4.8	1.99	0.81	2.47	326	403	0.81

[a] Toluene insoluble portion of the sample.

[b] Calculated from the chromatogram as linear polymer and corrected for instrumental spreading.

[c] Toluene solution (mL/g).

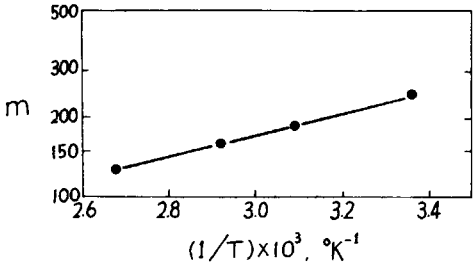

Fig. 6. Arrhenius plot of number of entanglement m against temperature ($1/T$) for Ln–PIR.

The molecular weight distribution of Ln–PIR whole sample was determined by gel permeation chromatography (GPC) using tetrahydrofurane as eluant. Similar measurements were carried out for a number of Ti–PIR whole samples for comparison. The GPC was calibrated by linear polyisoprene fractions of known weight average molecular weight as standards. The toluene insoluble portion of the sample was first determined as gel content, and the filtered toluene solution was subjected to viscosity measurement. Whole samples of polyisoprene were dissolved in tetrahydrofurane, and the solutions were filtered through a sintered glass filter on which a layer of anhydrous calcium sulfate (5–7 mm) was placed in order to remove the microgel particles. Average molecular weights and intrinsic viscosities of the samples calculated from the chromatograms and corrected for instrumental spreading are listed in Table I. $[\eta]_{GPC}$ (Table I) is calculated from $M(V_R)$ curve (not shown, where V_R refers to retention volume) and $[\eta](M)$ equation, so it represents $[\eta]$ in toluene solution, regardless of what kind of eluant was used. The normalized chromatograms of Ln–PIR(J) and two typical Ti–PIRs are shown in Figure 3.

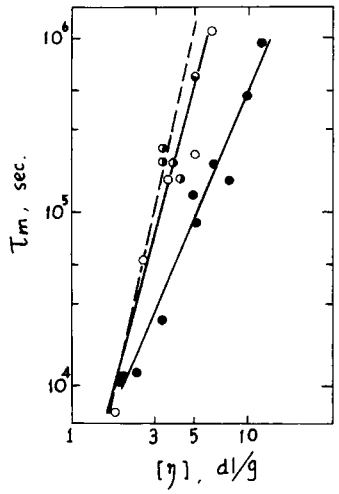

Fig. 7. Double logarithmic plot of max relaxation time τ'_m against intrinsic viscosity $[\eta]$ for PIRs: (●) Ln–PIR; (◑) Ti–PIR; (◒) Li–PIR; (○) NR; (—) experimental data; (- - -) calculated curve, $\gamma = \beta/\alpha = 3.4/0.7 = 4.86$.

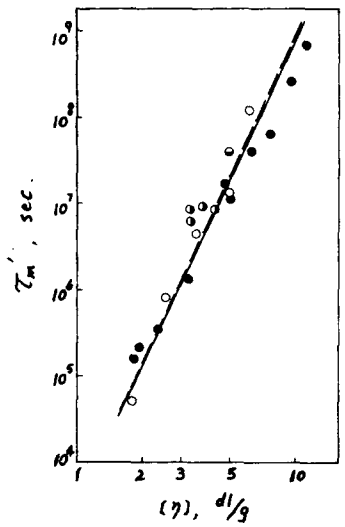

Fig. 8. Double logarithmic plot of reduced max. relaxation time τ'_m against intrinsic viscosity $[\eta]$ for PIRs: (●, ◑, ◒, ○) same as Figure 7; (—) reduced curve, slope $\gamma' = 4.64$; (- - -) calculated curve, slope $3.4/0.7 = 4.86$.

Among the samples investigated (Table I and Fig. 3) the Ln–PIR possesses the lowest gel content and the widest molecular weight distribution. On the other hand, the calculated intrinsic viscosity for Ln–PIR conforms with the experimental value while the calculated intrinsic viscosities for Ti–PIR are all higher than the experimental values. Since the GPC intrinsic viscosities are calculated on the basis of the calibration curve for linear poly-

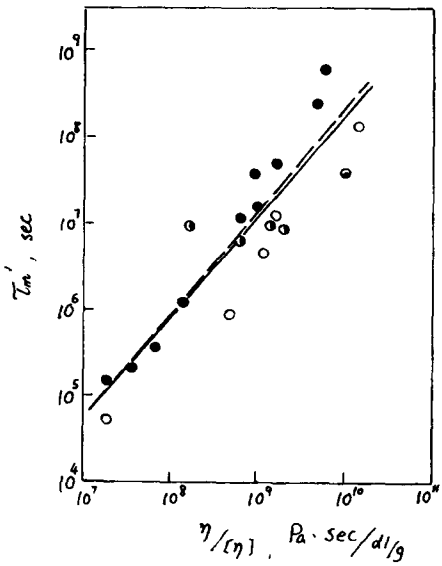

Fig. 9. Double logarithmic plot of reduced max relaxation time τ'_m against viscosity ratio $\eta/[\eta]$: (—) reduced curve, slope $\epsilon' = 1.18$; (- - -) calculated curve, slope $\gamma/(\delta/\alpha - 1) = 4.86/(3.4/0.7 - 1) = 1.26$.

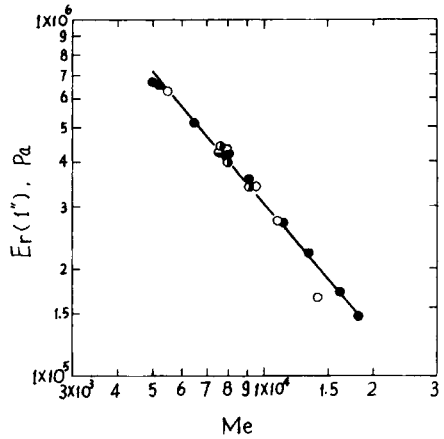

Fig. 10. Double logarithmic plot of relaxation modulus at 1-s $E_r(1'')$ against molecular weight of entanglement segment M_e: (○) NR; (◑) Ti-PIR; (◒) Li-PIR; (●) Ln-PIR.

mers, the ratio $\langle g \rangle_\eta = \langle [\eta] \rangle_{expt} / \langle [\eta] \rangle_{GPC}$ may be taken as an index for branching. The data indicate that branching is present in Ti-PIR(A) and is practically negligible in Ln-PIR(J).

STRESS-RELAXATION

Stress relaxation experiments for PIR specimens were carried out under isothermal constant stretching (50%) conditions at various temperatures ranging from 25–150°C.

The isothermal stress relaxation curves are reduced to a master curve at 25°C with various shift factors A_T, from which relaxation spectrum, bulk viscosity, etc., can be calculated. From the Arrhenius plot of log A_T against $1/T$ (Fig. 4), relaxation activation energy ΔE_{rel} for Ln-PIR is 42–50 kJ/mol, which is approximately twice as large as that for Ln-PB (21–34 kJ/mol).[3] The stress produced in Ln-PIR raw rubber is more difficult to relax than that in Ln-PB.

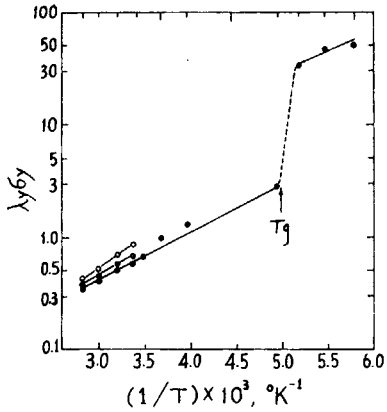

Fig. 11. Arrhenius plot of true yield strength $\lambda_y\sigma_y$ against temperature ($1/T$) for PIR; (●) Ln-PIR; (◑) Ti-PIR; (○) NR.

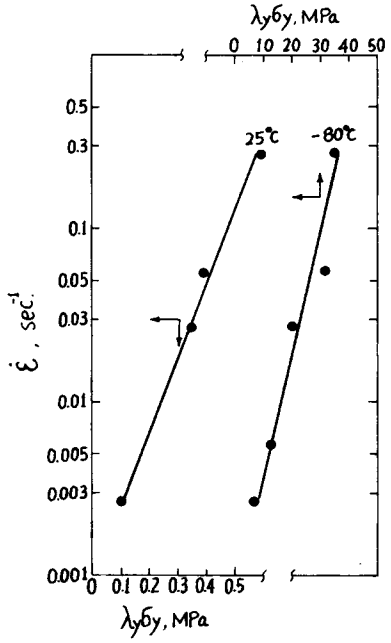

Fig. 12. Eyring plot of strain rate ($\dot{\epsilon}$) against true yield strength $\lambda_y\sigma_y$ for Ln–PIR below and above T_g

Entanglement

The number of entanglement segments m per molecule in bulk polymer can be estimated from the relaxation spectrum according to Chompff's approximation.[3] The calculated results show that the value of m increases exponentially with increasing M_η. By double logarithmic plotting m vs. M_η (Fig. 5), one may obtain the value of e from the following equation:

$$m = K_e M_\eta^e$$

for Ln–PIR e equals 1.48 (Table II). The critical molecular weight M_c for the onset of entanglement coupling can be obtained by extrapolating to $m = 1$, $M_{c\,(m=1)} = 5.28 \times 10^4$ for Ln–PIR, equivalent to $X_c = M_c/M_0 = 778$ monomeric units ($M_0 = 68$) per entanglement segment, nearly 1.7 times that for Ti–PIR and NR.

Such entanglement should be physical in nature and, therefore, dependent on temperature; it can be disentangled by increasing the temperature.

TABLE II
Dependence of Number of Entanglement Segment m on Viscosity Average Molecular Weight M_η, $m = K_e M_\eta^e$

Sample	e	K_e	$M_{c(m=1)}$	$X_c = M_c/M_0$
Ln–PIR	1.48	1.05×10^{-7}	5.28×10^4	778
Ti–, NR	1.43	3.70×10^{-7}	3.14×10^4	462

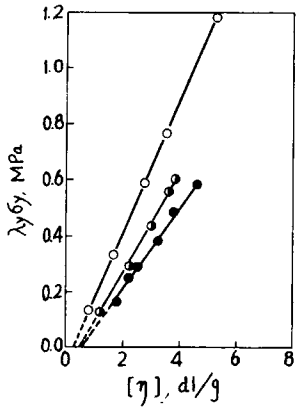

Fig. 13. Dependence of true strength $\lambda_y\sigma_y$ (25°C, 500 mm/min) an intrinsic viscosity $[\eta]$ (30°C, toluene); (○) NR; (◑) Ti-PIR; (●) Ln-PIR.

By Arrhenius plotting of log m vs. $1/T$ (Fig. 6), one can obtain the activation energy of disentanglement ΔE_{deN}, which equals 8.0 kJ/mol.

Maximum Relaxation Time Relating to Branching and Entanglement

Maximum relaxation time τ_m can be obtained from the master relaxation curve. It is dependent on molecular weight or $[\eta]$ to γth power,[2]

$$\tau_m = K_\gamma[\eta]^\gamma$$

The value of γ is correlated to the extent of branching and entanglement. The γ value for Ln-PIR is 2.42 (Fig. 7 and Table III), equivalent to the value 2.41 for Ln-PB.[2] The macromolecules of Ln-PB are linear, but the molecular weight distribution is broad. The presence of very high molecular weight fractions will cause entanglement. On the other hand, the γ value for Ti-PIR and NR is 3.58, close to 3.62 for Ni-PB, the latter is branched,[2] and the branched macromolecules are readily entangled too (Fig. 5). If we take the number of entanglements M_η/M_e as a reduction factor, similar to that stated by Graessley et al.,[4] and let the reduced maximum relaxation time $\tau'_m = (M_\eta/M_e) \cdot \tau_m$, the dependence of τ'_m on M_w should then be close to the

TABLE III
Dependence of Maximum Relaxation time τ_m on Intrinsic Viscosity $[\eta]$[a]

Sample	α	γ	β
Ln-PIR	0.70	2.42	1.7
Ti-NR	0.67	3.58	2.4
Reduced	0.70	$\gamma' = 4.64$	3.25
Calculated	0.70	4.86	3.4

[a] $\left.\begin{matrix}\tau_m = K_\beta M_w^\beta \\ [\eta] = K_\alpha M_w^\alpha\end{matrix}\right\} \Rightarrow \tau_m = K_\gamma[\eta]^\gamma,\ \gamma = \beta/\alpha.$

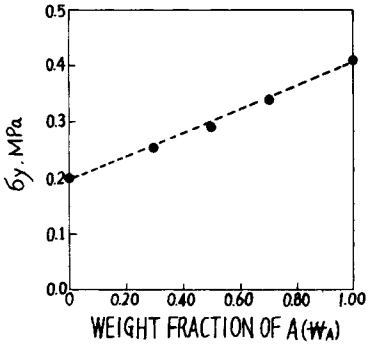

Fig. 14. Additivity of yield strength σ_y for Ln-PIR, $\sigma_y = W/_A\sigma_{yA} + W/_B\sigma_{yB}$: (●) experimental value; (- - -) calculated line.

3.4th power law. The two lines (Fig. 8) with different slopes (Fig. 7) are reduced or normalized into one; its slope γ' is 4.64, very close to $\gamma' = 3.4/0.7 = 4.86$.

The entanglement reduction method can be extended to the case for evaluating the molecular weight dependence on bulk viscosity $\eta(M)$,

$$\eta = K_\delta M_w^\delta$$

while the value of η can be obtained from the master relaxation curve as $\eta = \tau G$, where G represents shear modulus. The value of the exponent δ ranges from 3 to 3.4 in theory and practice.

The ratio of bulk viscosity to intrinsic viscosity may be used as a measure of the degree of branching/entanglement. The physical meaning of the ratio is obvious since $\eta/[\eta] = K \cdot \bar{r}^2 m/M_e$, where r, m, and M_e represents end-to-end distance, number of entanglements per molecule, and molecular weight of entangled segment, respectively, which may be viewed as an indication of the degree of tightness of entanglement.[5] From the log–log plot of τ'_m

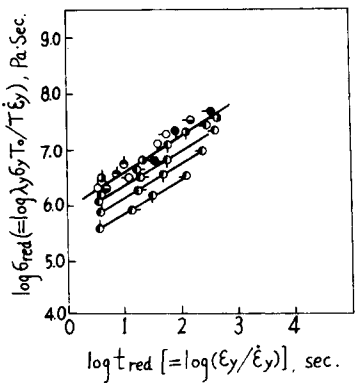

Fig. 15. Double logarithmic plot of reduced yield strength σ_{red} against reduced time t_{red} for Ln–PIR(J) series with different molecular weights; T (°C); $\dot{\epsilon}$ (s^{-1}): (○) 80, (○) 0.27; (●) 60, (○) 0.056; (◐) 40; (◐) 25, (○) 0.027; (◐) 15, (○) 0.0027; (◐) 0.

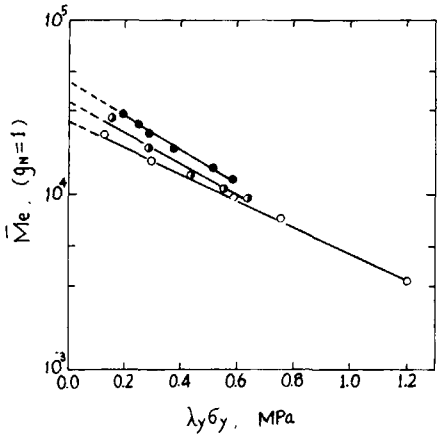

Fig. 16. Plot of molecular weight of entanglement segment $M_{e(q_N=1)}$ against true yield strength $\lambda_y\sigma_y$ for PIR: (●) Ln-PIR(J-O ~ 5); (◑) Ti-PIR(1220); (○) NR.

against $\eta/[\eta]$ (Fig. 9), all the experimental data of Ln-, Ti-PIR, and NR fall reasonably well on one straight line with a slope ϵ' of 1.18.

From the combination of the related equations, i.e., $[\eta] \infty M_w^{\alpha}$, $\tau_m' \infty [\eta]^{\gamma'}$, $\tau_m \infty (\eta/[\eta])^{\epsilon'}$ with $\eta \infty M_w^{\delta}$, we can get the value of

$$\delta = (\gamma'/\epsilon' + 1)\alpha = (4.64/1.18 + 1) \cdot 0.70$$
$$= 3.45$$

The experimental value agrees with the theoretical 3.4th power law. The entanglement reduction method is thus verified.

Dependence of Relaxation Modulus on the Molecular Weight of Entanglement Segment

The relaxation modulus at 1-s E_{rel} (1″) is dependent on η or M_η,[2] and the double-logarithmic plots for several kinds of synthetic PIR and NR are parallel straight lines.

If the molecular weight of entanglement segment M_e is functioned as a reduction factor, by plotting $\log E_{rel}(1'')$ vs. $\log M_e$ (Fig. 10) all the experimental data can be reduced to one straight line with a negative slope of -1.2 by the following equation:

$$E_{rel}(1'') = 2.67 \times 10^{10} M_e^{-1.2} \quad \text{(Pa)}$$

Regardless of synthetic Ln-, Ti-, and Li-PIR or natural PIR, i.e., irrespective of linear or branched chain and whether entanglements exist, the relaxation modulus at short interval is directly controlled by the length of entanglement segment M_e. A similar conclusion has been reached for Ln- and Ni-PB, of which the slope is also -1.2.[5]

YIELD STRENGTH

From the yield point on a stress–strain curve of high molecular weight raw rubber, the nominal yield strength σ_y, the yield deformation $\epsilon_y = \Delta l / l_0$ and the corresponding strain rate $\dot{\epsilon}_y = \mathrm{d}\,\epsilon_y/\mathrm{dt}$ can be determined. When

TABLE IV
Activation Energy ΔE_y and Activation Volume V_y for Yielding Process[a]

ΔE_y or V_y	Sample	Rubbery (20°C)	Glassy (−80°C)
Activation energy, ΔE_y (kJ/mol)	Ln–PIR	8.4	6.8
	Ti–PIR	9.6	
	NR	11.7	
Activation volume V_y (nm^3)	Ln–PIR	15.4 (X_y = 136)	0.17 (X_y = 1.5)

[a] Arrhenius, $\lambda_y\sigma_y = K_y \exp(\Delta E_y/RT)$; Eyring, $d\epsilon_y/dt = K'_y \exp(V_y\lambda_y\sigma_y/RT)$.

a specimen is stretched isothermally with a tensile testing machine (Changchun DL-1000 B Model) from its initial length l_0 to the length at yield point l_y, the yield elongation ratio can be defined as $\lambda_y = l_y/l_0 = 1 + \epsilon_y$, and the true yield strength should be $\lambda_y\sigma_y$.

Yield Behavior

Since the yield process of a bulk rubber is kinetic in character, our experiments were carried out at constant rate of stretching and various temperatures (80–100°C). The activation energy of yield behavior ΔE_y may be obtained (Table IV) from an Arrhenius plot of true yield strength log ($\lambda_y\sigma_y$) against $1/T$ (Fig. 11). For Ln–PIR in rubbery state, ΔE_y = 8.4 kJ/mol, in agreement with ΔE_{deN} = 8.0 kJ/mol, as obtained independently by stress–relaxation methods. Therefore, the yield of a raw rubber under stress is actually a process of loosening physical entanglements among macromolecular chains.

On further quenching to the glassy state, the yield strength increased abruptly as expected, while ΔE_y decreases approximately by 20%; here the potential barrier to be overcome may be a very small domain instead of the original one in the rubbery state.

With experiments at constant temperature and various rates (0.27–0.0027 s^{-1}) of extension, according to Eyring's viscosity theory for yield process, the activation volume V_y can be obtained by plotting strain rate log $\dot{\epsilon}$ against strength $\lambda_y\sigma_y$ (Fig. 12). Assuming this to be the volume of moving segment during the occurrence of yield deformation, the corresponding number of yielding segment can be estimated by this equation $X_y = V_y\rho N/M_0$, where ρ is the density (0.91 g/mL), N is Avogadro's number, and M_0 is the molecular weight of monomeric unit. Activation volume of Ln–PIR rubber is found to be 15 nm^3, corresponding to 136 monomeric units (Table IV) being disturbed on yielding at room temperature. When the specimen was quenched from rubbery state to glassy state, it only affected a very small domain, corresponding to 1.5 units.

Dependence of Yield Strength on Molecular Weight

In the case of PB raw rubber, there is a linear relationship between yield strength and molecular weight.[2,6] It is further confirmed in the case of PIR rubber (Fig. 13, Table V) that

$$\lambda_y\sigma_y = A[\eta] + B \quad (\sigma_y \text{ in MPa, } [\eta] \text{ in dL/g})$$

TABLE V
Dependence of Yield Strength σ_y on Molecular Weight M_η or $[\eta]$ for PIRs $\lambda_y\sigma_y = A[\eta] + B$

PIR	A	$-B$	Critical value at $\sigma_y = 0$		
			$[\eta]_c$ (dL/g)	$M_c \times 10^{-4}$	$X_c = M_c/M_0$ (d)
Ln–PIR	0.14	0.05	0.37	5.7[a]	840
Ti–PIR	0.18	0.08	0.45	7.6[a]	1100
				4.0[b]	590
NR	0.24	0.06	0.27	1.4[c]	210

[a] $[\eta] = 1.73 \times 10^{-4} M_w^{0.70}$ (this paper).
[b] $[\eta] = 2.0 \times 10^{-4} M_w^{0.728}$ [W. H. Beattie, and C. J. Booth, *Appl. Polym. Sci.*, **7**, 507 (1963)].
[c] $[\eta] = 5.02 \times 10^{-4} M_w^{0.67}$ [see, e.g., D. W. Fraga, *J. Polym. Sci.*, **41**, 522 (1959)].
[d] M_0 of $C_5H_8 = 68$.

For Ln–PIR, $A = 0.14$ and $B = -0.05$. By extrapolation of σ_y approaching zero, the critical value of molecular weight for the occurrence of yield process, $M_c(\sigma_y = 0) = 5.7 \times 10^4$ may be obtained, equivalent to 840 monomeric units per yielding segment. This value agrees well with $M_{c(m=1)} = 5.28 \times 10^4$, which is obtained by the stress–relaxation method.

However, such a relationship exists only in the rubbery state, but not in the glassy state (Table VI). The yield strengths at -103°C of three Ln–PIR samples with different molecular weights are all equal to 20 kg/cm^2.

Since the yield strength is dependent on $[\eta]$, and $[\eta]$ is additive in nature, σ_y should also be additive,[2] i.e., $\sigma_y = \epsilon W_i \sigma_{ji}$. When two samples of PIR rubber with different molecular weights and yield strengths are blended in different weight proportions (W_i), as expected, the experimental results agree very well with the calculated line (Fig. 14).

Critical Molecular Weight Estimated by Reduced Yield Strength Method

The relation between yield stress and yield strain is treated by Ferry's reduction method according to Smith.[7] The reduced curve can be constructed by double logarithmic plot of reduced strength per unit stretching rate $\sigma_{red} = \lambda_y \sigma_y T_0/\dot{\epsilon}_y T$ against reduced time $t_{red} = \epsilon_y/\dot{\epsilon}_y$. The plots in Figure 15 are for a series of Ln–PIR(J-0–5) with different molecular weights. The slope of the reduced line may approximates the equilibrium modulus due to entanglement E_{eN} of the rubbery plateau, according to the theory of rubber elasticity,

$$E_{eN} = 3g_N \rho RT/M_e$$

TABLE VI
Yield Strength σ_y for PIR at Rubbery and Glassy State

$[\eta]$ (dL/g)	Nominal Yield Strength (kg/cm^2)	
	Rubbery (25°C)	Glassy (-80°C)
4.6	1.7	20
6.8	2.8	20
9.5	4.4	21

The molecular weight of entanglement segment M_e can be estimated by proper choice of the value of g_N, which usually ranges from 0.5 to 1.0, but Pearson[8] obtained a value of 1.22 for PB. By plotting log $M_e(g_N = 1)$ against $(\lambda_y\sigma_y)$, the straight lines in Figure 16 may be expressed as

$$\log M_e = C(\lambda_y\sigma_y) + D$$

The results are listed in Table VII, for the Ln–PIR(J-0–5) series $C = -0.99$ and $D = 4.64$. By extrapolation, we obtain the critical value $M_c(\sigma_y = 0, g_N = 1.22) = 5.4 \times 10^4$, just lying between the values of $M_{c(m=1)} = 5.28 \times 10^4$ and $M_{c(\sigma_y=0)} = 5.7 \times 10^4$. The average value of M_c may be taken as $(5.4 \pm 0.2) \times 10^4$ for Ln–PIR.

CONCLUSIONS

The *cis*-1,4 content in polyisoprene raw rubbers polymerized with lanthanide catalyst system (Ln–PIR) equals from 93 to 96.x% with mixed lanthanides used as catalyst.

The viscosity $[\eta]$ equation for molecular weight M_w of Ln–PIR is $[\eta] = 1.73 \times 10^{-2} M_w^{0.70}$ (mL/g, toluene, 30°C). There is practically no branching in the macromolecular chains, and its molecular weight distribution is rather broad.

The number of entanglement segments m deduced from relaxation spectrum is dependent on molecular weight; the critical molecular weight for the onset of entanglement $M_{c(m=1)}$ is 5.28×10^4. The activation energy for disentanglement ΔE_{deN} is determined as 8.0 kJ/mol, while the ΔE_y for the start of yielding is 8.4 kJ/mol.

For PIR rubbers, including Ln–PIR, Ti–PIR, and natural rubber, either linear or branched, the dependence of maximum relaxation time on $[\eta]$ can be normalized by introducing the number of entanglement M_η/M_c as a reduction factor. Such entanglement reduction method is verified by the molecular weight dependence on bulk viscosity $\eta(M)$ to a 3.45th power.

The relaxation modulus at 1-s $E_{rel}(1'')$ is controlled by the length of entanglement segment M_e, which is used as a reduction factor in $E_{rel}(1'') = 2.67 \times 10^{10}/M_e^{1.2}$ (Pa, 25°C).

PIR raw rubbers with high molecular weight exhibit yield strength, which depends on molecular weight, and possesses the nature of additivity. The critical molecular weight for the occurrence of yielding $M_c(\sigma_y = 0)$ is about

TABLE VII
Critical Molecular Weight M_c for Yielding Estimated from log M_e vs. $\lambda_y\sigma_y$ Plot for PIRs[d]

			$M_c(\sigma_y = 0, g_N) \times 10^{-4}$		
Sample	$-C$	D	$g_N = 1.0$	$g_N = 1.22$	
Ln–PIR	0.99	4.64	4.4[a]	5.4	($X_c = M_c/M_0 = 800$)
Ti–PIR	0.92	4.49	3.1[b]	3.8	(560)
NR	0.79	4.40	2.5[c]	3.1	(450)

[a,b,c] Same as Table V.

[d] $M_e = 3g_N\rho RT/E_{eN}$, log $M_e = C(\lambda_y\sigma_y) + D$

5.7×10^4. M_c can be estimated by the reduced yield strength method, $M_{c(\sigma_y = 0,\, g_N = 1.22)} = 5.4 \times 10^4$, just between the values of $M_{c(m=1)}$ and $M_{c(\sigma_y = 0)}$.

References

1. Shen Zhiquan, Ouyang Jun, Wang Fusong, Hu Zhenya, Yu Fusheng, and Qian Baogong, *J. Polym. Sci., Polym. Chem. Ed.*, **18**(12), 3345–3357 (1980).

2. Qian Baogong, Yu Fusheng, Chen Rongshi, Qin Wen, and Zhou Enle, *Proceedings of China–U. S. Bilateral Symposium on Polymer Chemistry and Physics* (Oct. 5–10, 1979, Beijing), Science Press, Beijing, Reinhold, New York, 1981, pp. 155–170. National Award for Natural Science (Oct. 1982, Beijing), China.

3. A. J. Chompff and J. A. Duisier, *J. Chem. Phys.*, **45**, 1505 (1966).

4. W. W. Graessley, R. L. Hazleton, and L. R. Lindeman, *Trans. Soc. Rheol.*, **11**, 267–285 (1967).

5. Zhang Yanshou and Qian Baogong, *Collected Pap. Changchun Inst. Appl. Chem.*, **17**, 36 (1981).

6. Yu Fusheng, Yan Yuhua, Li Shentian, and Qian Baogong, *Collected Pap. Changchun Inst. Appl. Chem.*, **18**, 1 (1982).

7. T. L. Smith, *J. Polym. Sci.*, **20**, 94 (1950).

8. D. S. Pearson, B. J. Shutnik, and G. G. A. Bohm, *J. Polym. Sci., Polym. Phys. Ed.*, **12**, 925 (1974).

Received September 24, 1981
Accepted May 23, 1984